Impact of band gap shrinkage on simulated bifurcation routes in directly modulated semiconductor lasers

C. G. Lim, S. Iezekiel, and C. M. Snowden

Citation: Journal of Applied Physics **99**, 043101 (2006); doi: 10.1063/1.2173308
View online: http://dx.doi.org/10.1063/1.2173308
View Table of Contents: http://scitation.aip.org/content/aip/journal/jap/99/4?ver=pdfcov
Published by the AIP Publishing

Impact of band gap shrinkage on simulated bifurcation routes in directly modulated semiconductor lasers

C. G. Lim[a)]
Department of Photonics/Institute of Electro-Optical Engineering, National Chiao Tung University, 1001 Ta Hsueh Road, Hsinchu 30010, Taiwan, Republic of China

S. Iezekiel
School of Electronic and Electrical Engineering, The University of Leeds, Leeds LS2 9JT, England

C. M. Snowden
University of Surrey, Surrey GU2 7XH, England

(Received 20 April 2005; accepted 16 January 2006; published online 24 February 2006)

A carrier heating model is derived by taking into account the various temperature processes in the active layer of laser diodes. This model is then used to simulate the static and dynamic characteristics of a directly modulated 1.55 μm distributed-feedback laser diode. The calculated results are compared with the measured results of this device as obtained in an earlier work [H. F. Liu and W. F. Ngal, IEEE J. Quantum Electron. **29**, 1668 (1993)], and this reveals the significant impact of band gap shrinkage on simulated results. This study also shows that the carrier heating model is a self-consistent model that naturally describes the gain suppression phenomena in directly modulated laser diodes. © *2006 American Institute of Physics*. [DOI: 10.1063/1.2173308]

I. INTRODUCTION

The nonlinear behavior of directly modulated laser diodes (LDs), and, in particular, their chaotic dynamics, has been widely studied by using rate equation models.[1–13] However, where the measured nonlinear behavior of LDs has been compared with rate equation models, the comparison has only been conducted for relatively small numbers of selected points in the frequency-modulation index space. Indeed, the early work with rate equations predicted chaotic behavior which was not observed experimentally,[1–5] and this led to the introduction of a phenomenological nonlinear gain suppression factor to correctly model the damping.[7–12] Subsequently, the bias dependence of the nonlinear gain suppression factor[14,15] was incorporated and found to improve the agreement between simulated and measured results.[13] The latter studies have clearly shown that the optical gain governs the nonlinear behavior of LDs. It therefore follows that temperature would be expected to play a crucial role in modeling the dynamic behavior of LDs since the gain is a strong function of temperature. However, the effect of temperature on the simulated bifurcation routes to chaos in directly modulated semiconductor lasers has not been studied rigorously. To do so would require an additional rate equation to model the LD temperature, and all temperature-dependent terms should be changed accordingly. In this paper, a carrier temperature rate equation will be presented and used in conjunction with the carrier and photon rate equations to simulate the bifurcation route to chaos of a 1.55 μm distributed-feedback (DFB) LD. Calculated results will be compared to those simulated using the widely used single-mode rate equations as well as the measured results presented in Ref. 11.

[a)]Electronic mails: cglim@faculty.nctu.edu.tw and C.G.LIM@ieee.org

II. SIMULATION MODELS AND CONSIDERATIONS

The first step in formulating a carrier temperature rate equation is to consider the major physical causes of carrier heating in semiconductor lasers which are described as follows:

(1) Due to the energy difference between the cladding and the active layers in semiconductor lasers, injected carriers must release this excess energy in order to relax down to the lasing band. Excess energy is redistributed to carriers in the active layer by carrier-carrier scatterings, thus causing a rise in carrier temperature.
(2) Besides stimulating free carriers to recombine, photons can also be absorbed by free carriers (i.e., free-carrier absorption). This process causes the energies of absorbed photons to be transferred to free carriers, increasing their energy and hence their temperature.
(3) The Auger recombination process describes the absorption of the energy released from a nonradiative carrier recombination by a free carrier, which therefore gains excess energy. Thus the carrier temperature rate equation needs to account for the Auger recombination heating especially for long-wavelength LDs.
(4) Spontaneous and stimulated emissions are the results of the recombination of free carriers with below average energy. Therefore, the carrier reservoir in the active layer is deprived of its lowest energy carriers, causing the average carrier energy and temperature to change.
(5) Finally, heated carriers relax their excess energy to longitudinal optical phonons and acoustic phonons.

Taking the above processes into account, the carrier temperature rate equation (in its general form) is formulated as

$$\frac{dT_e}{dt} = \frac{dT_{\text{inj}}}{dt} + \frac{dT_{\text{fca}}}{dt} + \frac{dT_{\text{Auger}}}{dt} - \frac{T_e - T_L}{\tau_\epsilon} - \frac{dT_{\text{spon}}}{dt} - \frac{dT_{\text{stim}}}{dt}, \tag{1}$$

where T_e and T_L are the average carrier temperature and lattice temperature, respectively, T_{inj}, T_{fca}, T_{Auger}, T_{spon}, and T_{stim} are the contributing temperature terms due to the injection current, free-carrier absorption, Auger recombination, and spontaneous and stimulated emissions, respectively, and τ_ϵ is the carrier energy relaxation time. In a more specific form, each of the above terms is modeled as in the following. The contribution of the injection current to the average carrier temperature is given by

$$\frac{dT_{\text{inj}}}{dt} = \left(\frac{\eta_i I/e}{NV}\right) E_{\text{inj}}, \tag{2}$$

where η_i is the internal quantum efficiency, I the injection current, e the electronic charge, N the carrier density, V the volume of the active layer, and E_{inj} the energy of an injected carrier. Free-carrier absorption heating is modeled as

$$\begin{aligned}\frac{dT_{\text{fca}}}{dt} &= \frac{v_g \alpha_{\text{fca}} SVE}{NV} \\ &= \frac{v_g \alpha_{\text{fca}} SE}{N},\end{aligned} \tag{3}$$

where v_g is the group velocity, α_{fca} the free-carrier absorption coefficient, S the photon density, and E the energy of emitted photons. The Auger recombination is significant in long-wavelength LDs and its contribution to the carrier temperature is described by

$$\frac{dT_{\text{Auger}}}{dt} = \left(\frac{CN^3V}{NV}\right) E_g = CN^2 E_g, \tag{4}$$

where C is the Auger recombination coefficient and E_g the band gap energy. Spontaneous and stimulated emissions remove electrons from the conduction band edge thus reducing the free-electron energy. These affect the average carrier temperature and their contributions can be calculated using the following:

$$\begin{aligned}\frac{dT_{\text{spon}}}{dt} &= \frac{T_{e(t)} - T_{e(t-\delta t)}}{\delta t} \\ &= \frac{(T_e NV - BN^2 V \delta t E)/(NV) - T_e}{\delta t} \\ &= \frac{T_e - BN\delta t E - T_e}{\delta t} \\ &= -BNE,\end{aligned} \tag{5}$$

$$\begin{aligned}\frac{dT_{\text{stim}}}{dt} &= \frac{T_{e(t)} - T_{e(t-\delta t)}}{\delta t} \\ &= \frac{(T_e NV - v_g GSV \delta t E)/(NV) - T_e}{\delta t} \\ &= \frac{T_e - (v_g GS\delta t E)/N - T_e}{\delta t} \\ &= -\frac{v_g GSE}{N},\end{aligned} \tag{6}$$

where B is the bimolecular recombination coefficient and G the optical gain. Gathering all contributing temperature terms and substituting them into Eq. (1) yield the following carrier heating model, which is combined with the single-mode rate equations:

$$\frac{dN}{dt} = \frac{\eta_i I}{eV} - AN - BN^2 - CN^3 - v_g GS, \tag{7}$$

$$\frac{dS}{dt} = \Gamma v_g GS - \frac{S}{\tau_p} + \Gamma \beta BN^2, \tag{8}$$

$$\begin{aligned}\frac{dT_e}{dt} = \left(\frac{\eta_i I/e}{NV}\right) E_{\text{inj}} + \frac{v_g \alpha_{\text{fca}} SE}{N} + \frac{v_g GSE}{N} - \frac{T_e - T_L}{\tau_\epsilon} + BNE \\ + CN^2 E_g,\end{aligned} \tag{9}$$

where A is the nonradiative recombination coefficient, Γ the optical confinement factor, τ_p the photon lifetime, and β the spontaneous emission factor. The optical gain model that goes with the above carrier heating model is

$$G(E) = \left(\frac{e^2 h |M_b|^2}{4\pi^2 \epsilon_o m_o^2 cnE}\right)\left(\frac{2m_r}{\hbar^2}\right)^{3/2} (E - E_g)^{1/2} f_c(E_c) f_v(E_v), \tag{10}$$

where h is Planck's constant, $\hbar$ reduced Planck's constant, n the refractive index of the active layer, c the speed of light in vacuum, ϵ_o the permittivity of free space, m_o the free-electron mass, m_r a mass ratio, $|M_b|^2$ the average matrix element for the Bloch states, $f_c(E_c)$ the occupation probability of an electron with the energy E_c, and $f_v(E_v)$ the occupation probability of a hole with the energy E_v.

In addition to carrier density variations, current-induced heating will also cause the refractive index of the active layer to change. Hence these phenomena will also lead to changes in the lasing wavelength, optical gain, and group velocity, and they are taken into consideration as follows:

$$\delta\lambda = \delta\lambda_N + \delta\lambda_T = (2\Lambda)\delta N\left(\frac{dn}{dN}\right) + \delta T\left(\frac{d\lambda}{dT}\right), \tag{11}$$

$$\delta n = \delta n_N + \delta n_T = \delta_N\left(\frac{dn}{dN}\right) + \left(\frac{1}{2\Lambda}\right)\delta T\left(\frac{d\lambda}{dT}\right), \tag{12}$$

where $\delta\lambda$ is the overall wavelength shift, $\delta\lambda_N$ the carrier-induced wavelength shift, $\delta\lambda_T$ the wavelength shift caused by current-induced heating, Λ the corrugation periodicity, δN the change in carrier density, dn/dN the rate of change in refractive index with carrier density, δT the temperature change, $d\lambda/dT$ the rate of change in emission wavelength with temperature, δn the overall refractive index change, δn_N the change in refractive index caused by carrier density variations, and δn_T the change in refractive index caused by current-induced heating.

TABLE I. Parameter values of a 1.55 μm InGaAsP distributed-feedback (DFB) semiconductor laser.

Parameter (symbol)	Value
Volume of active layer (V)	6.75×10^{-17} m^3
Photon lifetime (τ_p)	1.75 ps
Optical confinement factor (Γ)	0.35
Differential gain (g')	1.36×10^{-20} m^2
Group velocity (υ_g)	8.43×10^{7} m s^{-1}
Gain suppression factor (ϵ)	10^{-23} m^3
Transparent carrier density (N_t)	0.9×10^{24} m^{-3}
Nonradiative recombination coefficient (A)	10^{8} s^{-1}
Bimolecular recombination coefficient (B)	1.25×10^{-18} m^3 s^{-1}
Auger recombination coefficient (C)	3.5×10^{-41} m^6 s^{-1}
Spontaneous emission factor (β)	8×10^{-7}
Band gap shrinkage rate	0.325 meV/K
Free-carrier absorption rate	2.81×10^{3} s^{-1}
Carrier-induced index change	-1.8×10^{-26} m^3
Current-induced heating wavelength shift	0.09 nm/°C
Linewidth enhancement factor (α_H)	6

As for the work on simulating the nonlinear dynamics of directly modulated LD using conventional single-mode rate equations [i.e., (7) and (8)], the following gain model was used:

$$G(E)=\frac{g'(N-N_t)}{(1+\epsilon S)}, \tag{13}$$

where g' is the differential gain, N_t the carrier density at transparency, and ϵ the nonlinear gain suppression factor.

III. RESULTS AND DISCUSSIONS

In this section, the nonlinear dynamics of a directly modulated 1.55 μm DFB LD having the parameters shown in Table I will be studied numerically. Simulations using the conventional single-mode rate equations will be presented followed by simulations based on the carrier heating model developed in this work. As can be seen from the measured *L-I* curve (from Ref. 11) in Fig. 1, a good range of bias currents to study the nonlinear behavior of the DFB LD is around 20 mA since the DFB LD has a threshold current of 16 mA. Hence, in this study, bias currents of 18, 20, and 22 mA are used. These values were also used in Ref. 11 where a detailed experimental investigation of the bifurcation routes to chaos of the directly modulated DFB LD was performed.

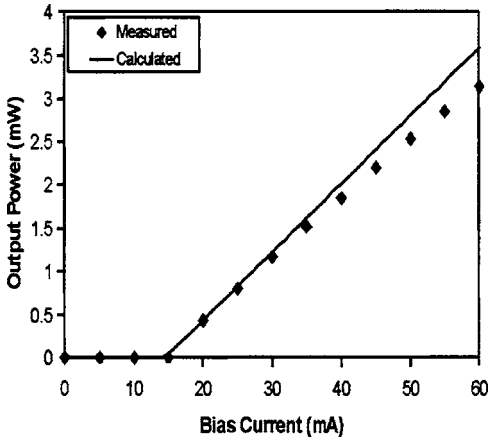

FIG. 1. Measured and calculated *L-I* curves of the 1.55 μm DFB LD. The calculated *L-I* curve was produced by the conventional single-mode rate equations, and the measured *L-I* curve is from Ref. 11.

A comparison of the calculated bifurcation behavior as shown in Fig. 2 with the measured results reported in Ref. 11 reveals that discrepancies exist over a large range of modulation frequencies at lower bias currents. At higher bias currents, the discrepancies are reduced and occur only at higher modulation frequencies. The above discrepancies will not be dealt with here as it has already been illustrated that a slight change in the optical gain has a significant effect on simulated results and that the reliability of the conventional single-mode rate equations in predicting the nonlinear behavior of directly modulated LDs can be improved by taking the injection current dependence of the gain suppression factor into consideration.[13] The initial carrier heating model results in Fig. 3 show suppression of period tripling and bear little resemblance to the measured data in Ref. 11. Nevertheless, the calculated results in Fig. 3 tend to match the measured results at higher bias currents, as do the results from the conventional single-mode rate equations. However, a noted difference between these two cases is that the correctly predicted bifurcation routes occur at slightly lower modulation frequencies for all three bias currents, whereas for the conventional model, this was only observed for a bias current of 20 mA. The above observations gave indications that the optical gain was not properly accounted for in the initial simulations, and that the computed optical gain for the carrier heating-based model is slightly higher than the actual optical gain. Hence, the optical gain produced by the gain model shown in (10) will be investigated below.

It is observed from the gain spectra calculated at various temperatures [Fig. 4(a)] that the gain peak is suppressed as temperature increases. However, the shift in gain spectrum caused by band gap shrinkage is not present in Fig. 4(a) and this phenomenon is anticipated to have a significant effect on the simulated results as this has an influence on the calculated optical gain at the emission wavelength. To take the band gap shrinkage into account, an additional term can be added to the formula for calculating the photon energy,

$$E=h\left(\frac{c}{\lambda+\delta\lambda}\right)+\delta T\left(\frac{dE}{dT}\right), \tag{14}$$

where λ is the lasing wavelength and dE/dT the rate of change in photon energy with temperature. All parameters that are a function of n and E were changed accordingly as n and E change. As can be observed from the gain spectra calculated with the band gap shrinkage [Fig. 4(b)], the gain peak has now shifted to longer wavelength besides being suppressed by increasing temperature. Also, it is seen that there is a significant difference in the optical gain at the emission wavelength between the cases where band gap shrinkage effect has and has not been accounted for. This is clearly reflected in the calculated *L-I* curves (Fig. 5) where the case which did not consider band gap shrinkage showed a lower threshold current (12 mA instead of the measured

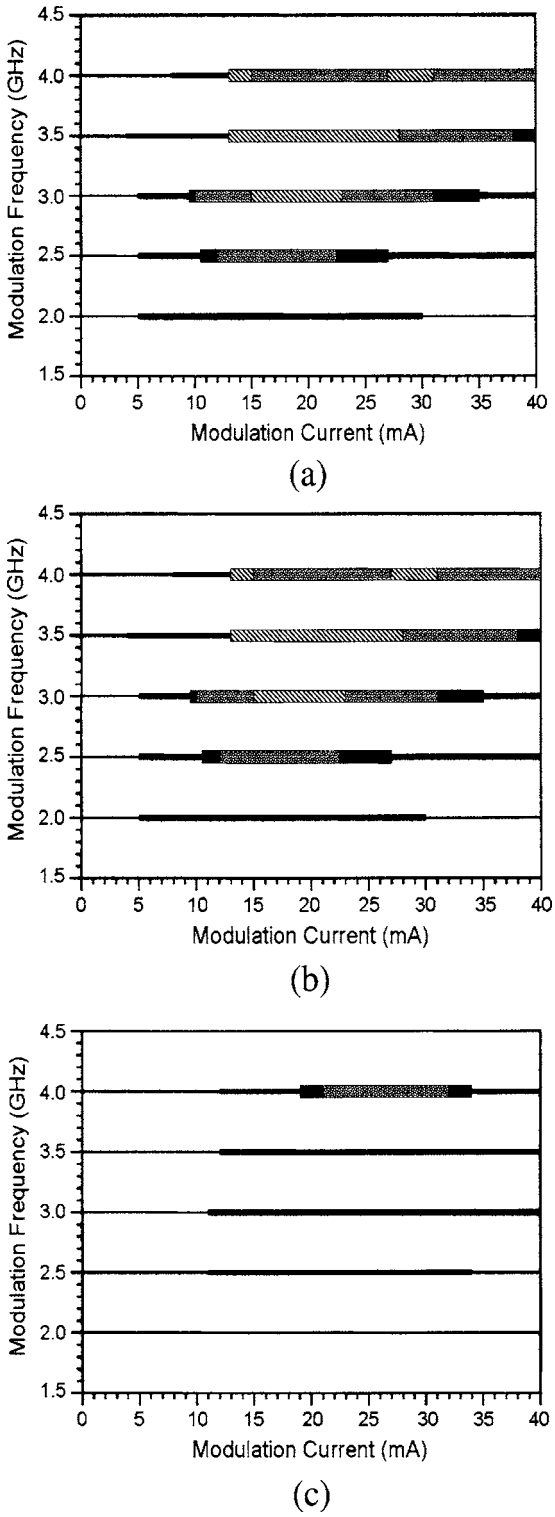

FIG. 2. Calculated bifurcation routes as produced by the conventional single-mode rate equations. (a) I_{dc}=18 mA, (b) I_{dc}=20 mA, and (c) I_{dc}=22 mA. [(—) single period, (■) period doubling (■) period tripling, (■) period quadrupling, and (■) chaos.]

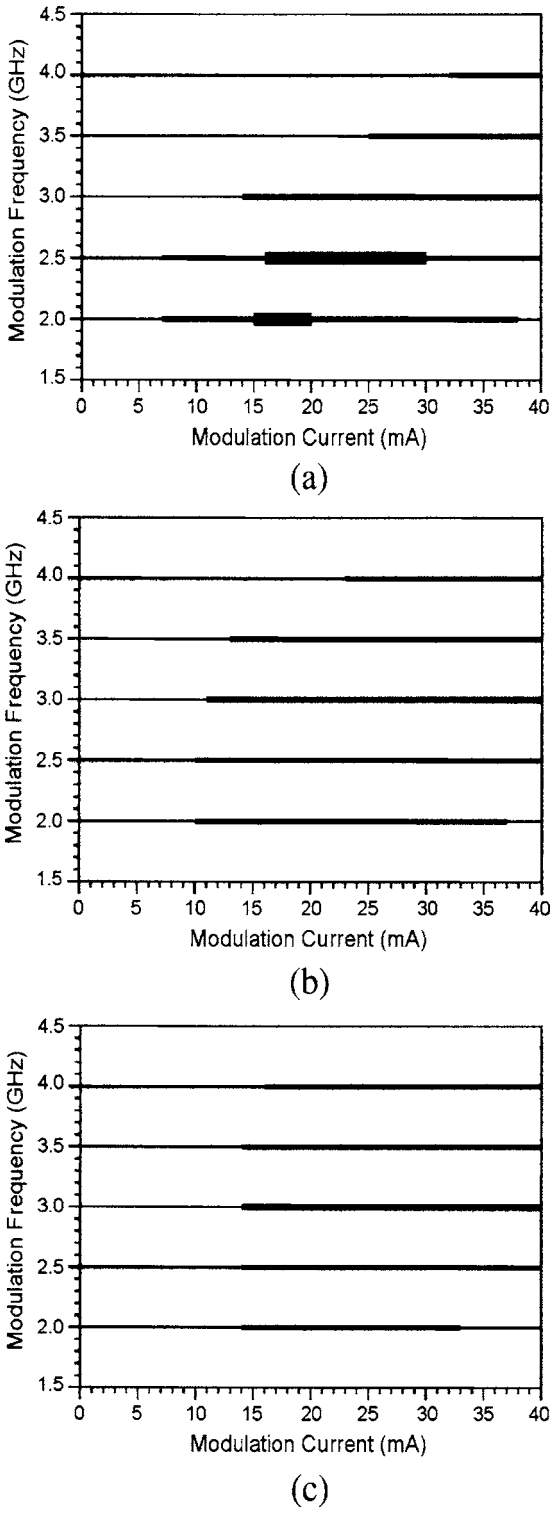

FIG. 3. Simulated bifurcation behavior based on the carrier heating model and the considerations as described in Sec. III. (a) I_{dc}=18 mA, (b) I_{dc}=20 mA, and (c) I_{dc}=22 mA. [(—) single period, (■) period doubling, and (■) period quadrupling.]

16 mA) and higher optical output powers than actually observed. When band gap shrinkage was accounted for, very good agreement between calculated and measured results was achieved, better than that produced by the conventional single-mode rate equations. Also noted was the effect of gain suppression due to the injection current heating when comparing the calculated *L-I* curve for the case where band gap shrinkage was not taken into consideration to the case where band gap shrinkage was taken into account. This is postulated to be the reason that the carrier heating model produces a *L-I* curve that agrees very well with measured result whereas the conventional single-mode rate equations do not. Analysis of the resulting simulated bifurcation routes (Fig. 6) and the measured results[11] yields the following observations:

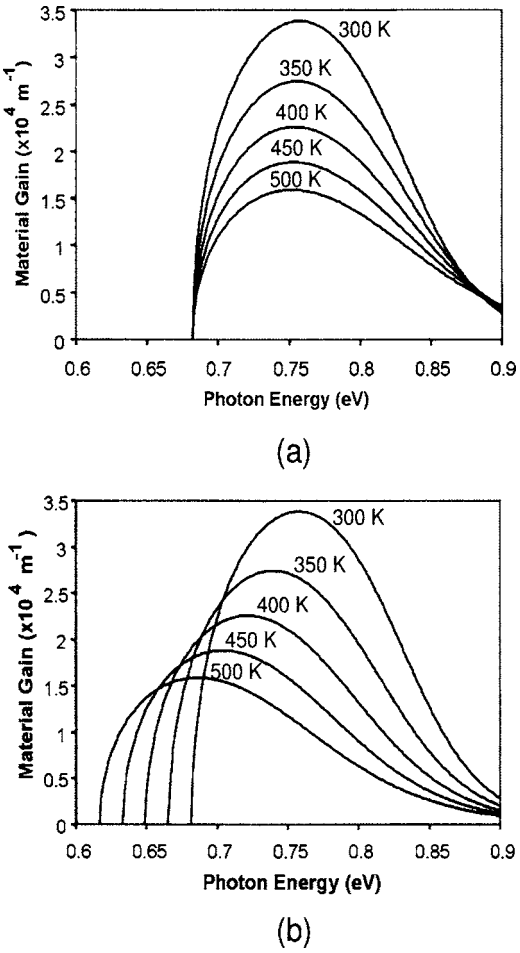

FIG. 4. Calculated gain spectra of the DFB LD at the threshold carrier density (i.e., 2.32×10^{24} m^{-3}). (a) Band gap shrinkage was not taken into consideration in the simulations. (b) Band gap shrinkage was accounted for in the simulations.

(i) I_{dc}=18 mA

(a) 2.5 GHz

The optical gain is lower than the actual value causing the simulation to produce the experimentally unobserved occurrence of chaos. Should the simulation produce a lower carrier temperature, chaos would not show up.

(b) 3.0 GHz

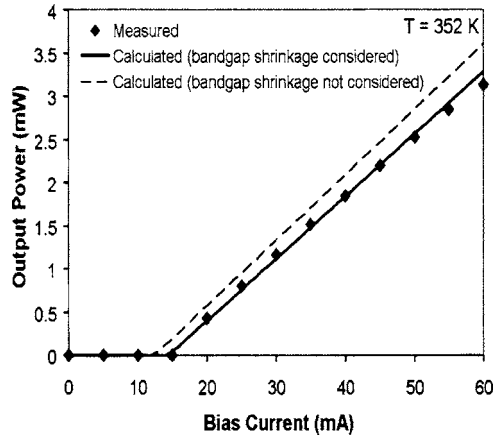

FIG. 5. Calculated *L-I* curves based on the carrier heating model. The measured *L-I* curve is from Ref. 11.

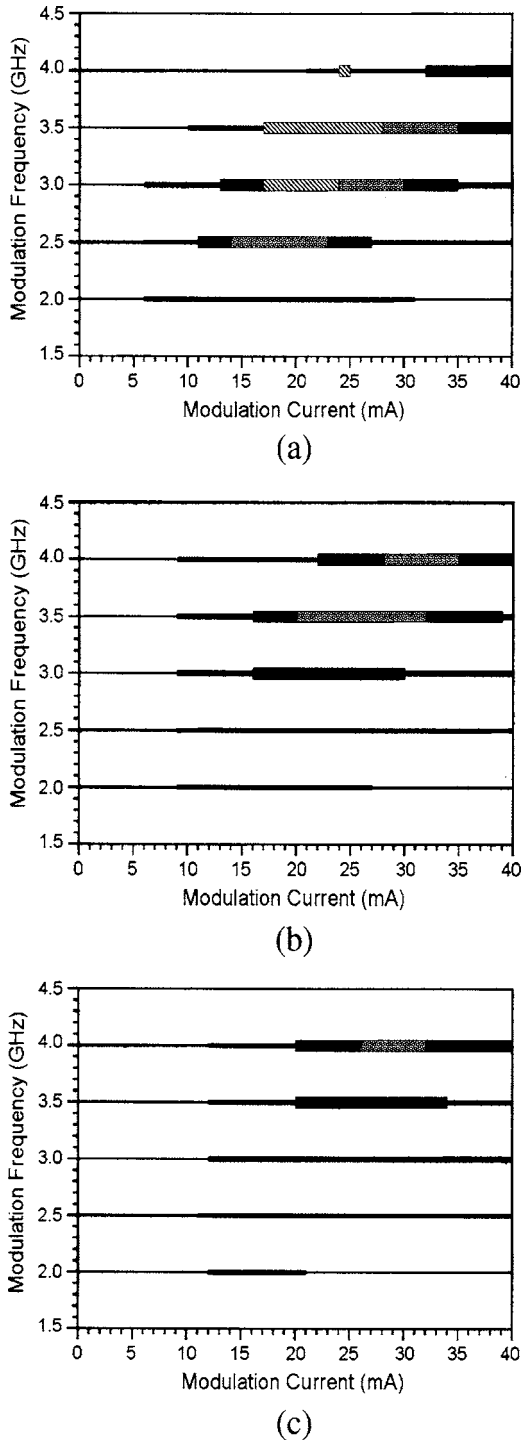

FIG. 6. Computed nonlinear behavior predicted by the carrier heating model whereby band gap shrinkage was taken into account. (a) I_{dc}=18 mA, (b) I_{dc}=20 mA, and (c) I_{dc}=22 mA. [(—) single period, (■) period doubling (■) period tripling, (■) period quadrupling, and (■) chaos.]

According to the measured result, this bifurcation route should occur at a modulation frequency of 3.5 GHz instead of 3.0 GHz. However, as the calculated carrier temperature is higher than the actual value, this gave rise to a lower optical gain and the simulation produced this measured bifurcation route at a slightly lower modulation frequency.

(c) 3.5 GHz

Similar to the above case where the modulation frequency was 3.0 GHz, the simulated bifurcation route is ac-

tually the measured bifurcation behavior at a modulation frequency of 4.0 GHz. Should the calculated optical gain be slightly higher, period quadrupling between the transition from period doubling to period tripling would have been produced in the simulation.

(d) 4.0 GHz

Judging from the above trend, probably this simulated bifurcation route would resemble the measured result at a modulation frequency of 4.5 GHz. However, measurement was not performed at modulation frequencies beyond 4.0 GHz.

(ii) $I_{dc}=20$ mA

For modulation frequencies of 2.0, 2.5, and 3.0 GHz, the calculated bifurcation route at each modulation frequency is actually the bifurcation behavior of that at 0.5 GHz higher according to measured results. However, due to the higher predicted carrier temperature the measured bifurcation behavior has shown up at a slightly lower modulation frequency.

(a) 3.5 GHz

This bifurcation route is actually that at a modulation frequency of 4.0 GHz if not for the small region of missing period tripling. The calculated carrier temperature is higher than the actual value causing the simulation to show a region of experimentally unobserved chaos instead of period tripling that was observed in the experiment.

(b) 4.0 GHz

Based on the above trend, the simulated bifurcation route at this modulation frequency is postulated to be that at a modulation frequency of 4.5 GHz which was not performed in experiment.

(iii) $I_{dc}=22$ mA

Similar to the simulated bifurcation behavior at bias currents of 18 and 20 mA, the trend that the measured bifurcation route occurring at a slightly lower modulation frequency in simulation has also shown up in this case, that is, the measured bifurcation route at modulation frequencies of 2.5, 3.0, 3.5, and 4.0 GHz occurred in the simulation at modulation frequencies of 2.0, 2.5, 3.0, and 3.5 GHz, respectively. As for the case where the modulation frequency was set at 4.0 GHz, it is postulated that the simulated bifurcation route should be that at a modulation frequency of 4.5 GHz.

From the observations, it is deduced that the discrepancies in simulated and measured bifurcation routes are caused by the slight discrepancies in simulated and measured modulation responses. As the above trend is also observed in the simulated bifurcation behavior obtained using the conventional single-mode rate equations, it is suspected that there is a slight discrepancy in the values of Γ, τ_p, β, A, B, or C. It could also be the effect of the accumulated discrepancy in the above parameters. Upon fixing the discrepancy in the value of the above parameters, it is expected that a good agreement between calculated and measured nonlinear behaviors of directly modulated LDs can be achieved by the carrier heating model in a self-consistent way. As for the conventional single-mode rate equations, it is possible to make this set of first-order ordinary differential equations a reasonably more self-consistent model by developing a rigorous model that accurately predicts gain suppression and relating it to photon density dynamically as proposed in Ref. 13. However, this is a very sophisticated approach because there are several processes that cause gain suppression at different rates, and each of these processes has different dominance under different conditions. To facilitate the development of a mathematical model for predicting the appropriate value for the gain suppression factor in any given condition, the carrier heating model developed here serves as an aid to study the gain suppression phenomena in details and relate it to the biasing condition and photon density. Consequently, this would lead to a single-mode rate equation model with an improved accuracy and self-consistency.

IV. CONCLUSIONS

Detailed numerical analyses based on the conventional single-mode rate equations and a carrier heating model were performed to study the nonlinear behavior of a directly modulated 1.55 μm DFB LD. Comparing the *L-I* curve produced by both models has shown that the *L-I* curve produced by the carrier heating model matches the measured result very well. The above good agreement between calculated and measured results was attributed to the fact that the carrier heating model accounts for the injection current heating. Results from this study have also shown that the optical gain suppression and gain-peak shift due to increased temperature (i.e., band gap shrinkage) have to be appropriately accounted for, otherwise the calculated optical gain at the emission wavelength will not be correct and this will lead to erroneous predictions of nonlinear behavior. Although a mathematical expression for the nonlinear gain suppression factor that takes into account the frequency-dependent phenomena mentioned in Ref. 13 could probably be derived through a rigorous study and used in conjunction with the conventional single-mode rate equations, this is a very complicated approach to treat the above mentioned frequency-dependent gain suppression phenomena. A fundamental approach has been taken in this study to investigate this matter. As a result, it has been shown that the frequency-dependent gain suppression phenomena mentioned above are not a concern to the computationally efficient and self-consistent carrier heating model proposed here. Hence, this carrier heating model serves as an effective and efficient study aid to gain insights on gain suppression phenomena. This would facilitate the development of a mathematical model for the gain suppression factor that would enhance the predictive power of the conventional single-mode rate equations.

[1]C. H. Lee, T. H. Yoon, and S. Y. Shin, Appl. Phys. Lett. **48**, 95 (1985).
[2]Y. C. Chen, H. G. Winful, and J. M. Liu, Appl. Phys. Lett. **47**, 208 (1985).
[3]M. Tang and S. Wang, Appl. Phys. Lett. **48**, 900 (1986).
[4]M. Tang and S. Wang, Appl. Phys. Lett. **50**, 1861 (1987).
[5]Y. Hori, H. Serizawa, and H. Sato, J. Opt. Soc. Am. B **5**, 1128 (1988).
[6]Y. G. Zhao, IEEE J. Quantum Electron. **28**, 2009 (1992).
[7]N. H. Jensen, P. L. Christiansen, and O. Skovgaard, IEE Proc.: Optoelectron. **135**, 285 (1988).
[8]L. Chusseau, E. Hemery, and J.-M. Lourtioz, Appl. Phys. Lett. **55**, 822 (1989).
[9]T. Y. Yoon, C. H. Lee, and S. Y. Shin, IEEE J. Quantum Electron. **25**, 1993 (1989).

[10]E. Hernery, L. Chusseau, and J. M. Lourtioz, IEEE J. Quantum Electron. **26**, 633 (1990).
[11]H. F. Liu and W. F. Ngal, IEEE J. Quantum Electron. **29**, 1668 (1993).
[12]G. P. Agrawal, Appl. Phys. Lett. **49**, 1013 (1986).
[13]C. G. Lim, S. Iezekiel, and C. M. Snowden, Appl. Phys. Lett. **78**, 2384 (2001).
[14]S. Schuster and H. Haug, Semicond. Sci. Technol. **10**, 281 (1995).
[15]Z. Toffano and A. Destres, Electron. Lett. **31**, 202 (1995).